Distribution of the distance between opposite nodes of random polygons with a fixed knot

2004 J. Phys. A: Math. Gen. 37 7993

(http://iopscience.iop.org/0305-4470/37/33/002)

INSTITUTE OF PHYSICS PUBLISHING JOURNAL OF PHYSICS A: MATHEMATICAL AND GENERAL

J. Phys. A: Math. Gen. **37** (2004) 7993–8006 PII: S0305-4470(04)77459-4

Distribution of the distance between opposite nodes of random polygons with a fixed knot

Akihisa Yao[1], Hiroshi Tsukahara[2], Tetsuo Deguchi[3] and Takeo Inami[1]

[1] Department of Physics, Faculty of Science and Engineering, Chuo University, 1-13-27 Kasuga, Bunkyo-ku, Tokyo 112-8551, Japan
[2] Geographic Information Systems Department, Hitachi Software Engineering Co., Ltd., 4-12-7 Higashishinagawa, Shinagawa-ku, Tokyo 140-0002, Japan
[3] Department of Physics, Faculty of Science, Ochanomizu University, 2-1-1 Ohtsuka, Bunkyo-ku, Tokyo 112-8610, Japan

Received 9 March 2004, in final form 7 June 2004
Published 4 August 2004
Online at stacks.iop.org/JPhysA/37/7993
doi:10.1088/0305-4470/37/33/002

Abstract

We examine numerically the distribution function $f_K(r)$ of the distance r between opposite polygonal nodes for random polygons of N nodes with a fixed knot type K. Here we consider three knots such as $\emptyset$, 3_1 and $3_1\sharp 3_1$. In a wide range of r, the shape of $f_K(r)$ is well fitted by the scaling form [1] of self-avoiding walks. The fit yields the Gaussian exponents $\nu_K = \frac{1}{2}$ and $\gamma_K = 1$. Furthermore, if we re-scale the intersegment distance r by the average size R_K of random polygons of knot K, the distribution function of the variable r/R_K should become the same Gaussian distribution for any large value of N and any knot K. We also introduce a fitting formula to the distribution $g_K(R)$ of gyration radius R for random polygons under some topological constraint K.

PACS numbers: 05.40.Fb, 61.25.Hg, 82.20.Wt, 02.40.Pc

(Some figures in this article are in colour only in the electronic version)

1. Introduction

Polymer chains in solutions or gels may be highly self-entangled: such entanglements should be important to understand some features of polymeric materials. A variety of knots can appear by connecting the two ends of a polymer chain. In fact, various knotted DNAs are synthesized in experiments through random closure of nicked DNA chains [2, 3]. Since topological questions were addressed by Delbrück [4], Frisch and Wasserman [5], several aspects of knotted ring polymers, such as the probability of random knotting [6–15], the average sizes [16, 17] and the complexity of their conformations [18] have been studied numerically and analytically.

Let us discuss the average size of knotted ring polymers with no excluded volume, i.e., the mean-squared gyration radius $R_K^2(N)$ of N-noded random polygons with fixed knot type K [19–25]. We consider random polygons as a simple model of ring polymers in solution at the θ-point [26]. At the θ-point polymers should have no effect of excluded volume. Furthermore, ring polymers keep their topology unchanged. It has now been established in simulations [20, 22–24] that the average size of random polygons with a fixed knot is larger than that with no topological constraint, when N is large. The topological swelling of random polygons may be explained in terms of entropic repulsion caused by the topological constraint. The phenomenon should be closely related to the 'topological excluded volume' proposed for such random polygons that possess the trivial knot $\emptyset$ [19]. Concerning the large-N behaviour of $R_K^2(N)$, however, the numerical studies do not unanimously arrive at the same conclusion. We have analysed the data of $R_K^2(N)$ for a model of random polygons [23], assuming the scaling formula of the following form:

$$R_K^2(N) = A_K N^{2\nu_K}(1 + B_K N^{-\Delta_K} + \cdots). \tag{1}$$

The result favours the interpretation $\nu_K = \nu_{\mathrm{SAW}}$. However, limiting the analysis to a narrower range of N, the alternative interpretation $\nu_K = \nu_{\mathrm{RW}}$ is also possible. Here, self-avoiding walks (SAW) and random walks (RW) have the scaling exponent $\nu_{\mathrm{SAW}} = 0.588$ and $\nu_{\mathrm{RW}} = 0.5$, respectively. Thus, in order to clarify the large-N behaviour of random polygons with fixed knots, it would be interesting to investigate some other quantity associated with the asymptotic behaviour.

In this paper, we study the following two quantities of random polygons with a fixed knot: (i) the distribution function of the distance between opposite nodes and (ii) the distribution of the radius of gyration. If the 'topological excluded volume' corresponds to a certain amount of excluded volume, then the distance between opposite nodes should follow a non-Gaussian distribution. For ring polymers with excluded volume, the distribution of the distance between opposite nodes should be non-Gaussian, while it is Gaussian for random polygons. Here we assume that the distance between opposite polygonal nodes plays the similar role as the end-to-end distance of a linear chain. For the self-avoiding walk, the end-to-end distance distribution is non-Gaussian [27, 28].

Through computer simulation of random polygons with fixed knots, we have evaluated the distributions of the distance r between opposite nodes of random polygons under the topological constraints [29]. We are concerned with the trivial knot, the trefoil knot and the composite knot consisting of two trefoil knots, which are denoted by $\emptyset$, 3_1 and $3_1\sharp 3_1$, respectively. We show that the scaling form of the self-avoiding walk gives good fitting curves to the data of the distributions in a wide range. It should be remarkable, since the scaling form of the end-to-end distance distribution is derived when $\rho = r/N^{\nu}$ is finite and very large [1, 27, 28, 30–34]. Furthermore, we show that the distribution function of the normalized distance r/R_K should be given by the same Gaussian form for any N and K. Here we recall that R_K denotes the average size of random polygons of knot K. Thus, it is suggested that the effect of the 'topological excluded volume' should be different from the standard excluded-volume effect.

We have also evaluated the distribution of the gyration radius for random polygons under some topological constraints [29]. We introduce a formula for describing the distribution, and discuss its fitting curves. The formula of the gyration-radius distribution is new, in particular, for random polygons under topological constraints. We note that for the Gaussian random walk, several approximate formulae of the gyration-radius distribution are known [35, 36].

The paper consists of the following. In section 2, we explain the model of random polygons, and define some symbols for the distribution functions. In section 3, we describe

briefly some procedures of the computer simulation. In section 4, we discuss the numerical results of this research. We plot the distribution function of the intersegment distance for random polygons under topological constraints. Through fitting curves to the data, we discuss that the distribution of the intersegment distance should be well approximated by the Gaussian distribution. We also plot the distribution of the gyration radius for random polygons under topological constraints. We thus investigate topological effects on the average sizes of random polygons. In section 5, we discuss that the 'topological excluded volume' should be different from the standard excluded volume, and present an open question.

2. Model and distribution functions

We consider a model of random polygons in which a polygon $\mathcal{P}_N$ consists of N line segments of length a. It is specified by position vectors of its nodes, $\mathcal{P}_N = (\boldsymbol{r}_1, \boldsymbol{r}_2, \ldots, \boldsymbol{r}_N)$. All cyclic permutations of the set of position vectors correspond to the same polygon. We recall that random polygons have no excluded volume. Hereafter we set $a = 1$.

When a polygon is topologically equivalent to a knot K, we call it a polygon of knot type K. The configuration space $\mathcal{C}$ of polygons is divided into subspaces $\mathcal{C}_K$ in which all polygons have the same knot K. We have $\mathcal{C} = \sum_K \mathcal{C}_K$.

For a polygon $\mathcal{P}_N$, we denote the intersegment vector from the ith node to the $(i + \lambda N)$th node

$$\boldsymbol{r}(i; \lambda, \mathcal{P}_N) = \boldsymbol{r}_{i+\lambda N} - \boldsymbol{r}_i, \tag{2}$$

where the progress parameter λ takes a value between 0 and 1. Here we assume the convention: $\boldsymbol{r}_{N+i} = \boldsymbol{r}_i$.

We define the distribution of the distance between the ith and the $(i + \lambda N)$th nodes by the probability $f(r; \lambda, N)\Delta r$ that the length of the intersegment vector $\boldsymbol{r}(i; \lambda, \mathcal{P}_N)$ takes a value between r and $r + \Delta r$:

$$f(r; \lambda, N)\Delta r = \frac{1}{NM} \sum_{m=1}^{M} \sum_{i=1}^{N} \int_r^{r+\Delta r} \mathrm{d}r\, \delta(r - |\boldsymbol{r}(i; \lambda, \mathcal{P}_{N,m})|). \tag{3}$$

Here Δr is a small positive real number. We choose it so that the statistical fluctuation of $f(r; \lambda, N)$ becomes moderately small. The distribution of the distance between two nodes for random polygons with a fixed knot type K is similarly defined by

$$f_K(r; \lambda, N)\Delta r = \frac{1}{NM_K} \sum_{m=1}^{M} \sum_{i=1}^{N} \int_r^{r+\Delta r} \mathrm{d}r\, \delta(r - |\boldsymbol{r}(i; \lambda, \mathcal{P}_{N,m})|)\chi(\mathcal{P}_{N,m}, K). \tag{4}$$

Here the indicator function $\chi(\mathcal{P}, K)$ filters the polygons of knot type K; it takes the value 1 if $\mathcal{P} \in \mathcal{C}_K$ and 0 otherwise.

We calculate the distribution $f(r; \lambda, N)$ of the intersegment distance r by randomly generating a large number of polygons $\mathcal{P}_{N,m}$ with length N for $m = 1, \ldots, M$. Here the subscript m denotes the mth polygon generated. The number of generated polygons of the knot type K is given by $M_K = \sum_m \chi(\mathcal{P}_{N,m}, K)$, and we have $M = \sum_K M_K$.

Let us denote the square of the gyration radius of a polygon $\mathcal{P}_N$ by

$$R_G^2(\mathcal{P}_N) = \frac{1}{2N^2} \sum_{i,j=1}^{N} (\mathbf{r}_i - \mathbf{r}_j)^2. \tag{5}$$

We define the distribution $g(R; N)$ for gyration radius R by

$$g(R; N)\Delta R = \frac{1}{M} \sum_{m=1}^{M} \int_R^{R+\Delta R} \mathrm{d}R\, \delta\big(R - \sqrt{R_G^2(\mathcal{P}_{N,m})}\big), \tag{6}$$

and the one for polygons with knot type K by

$$g_K(R; N)\Delta R = \frac{1}{M_K}\sum_{m=1}^{M}\int_R^{R+\Delta R} \mathrm{d}R\,\delta\big(R - \sqrt{R_G^2(\mathcal{P}_{N,m})}\big)\chi(\mathcal{P}_{N,m}, K). \quad (7)$$

3. Simulation procedure

A pivot move for a polygon is a rotation of a chain of segments, randomly chosen from the polygon, around the axis passing the two endmost nodes of the chain by a random amount of angle ϕ [23, 37]. The rotation angle ϕ is selected randomly from the interval between 0° and 360°. We do not check self-intersections during the process of rotation of the chain since such configurations are negligible in the space $\mathcal{C}$.

We start from a seed conformation placed on the cubic lattice, which is regarded as a special conformation of the off-lattice polygon in the continuum space [38]. We then generate a sequence of polygons by applying the pivot moves repeatedly. After discarding the initial 2000 transient conformations, we take samples of polygons at every 200 pivot moves.

To determine the topology of polygons, we employ two simple knot invariants. We calculate the special value of the Alexander polynomial $\Delta_K(t)$ at $t = -1$ [6] (which is also called the determinant of a knot), and the Vassiliev invariant of the second-order $v_2(K)$ [39, 40]. With these invariants, the chance of misidentification of topology class for a given polygon should be negligible and much smaller than the statistical errors of the data, as far as the simple knots are concerned.

The simulation has been performed for polygons with the length $N = 300$ and 600. We have generated $M = 3 \times 10^6$ random polygons for each given length N. We have classified those polygons into four groups according to their knot types, the three groups of polygons with the specific knot types $\emptyset$, 3_1 and $3_1\sharp 3_1$, and the other group of knot types other than the previous three. The three knots have distinct sets of values for the two knot invariants $|\Delta_K(t = -1)|$ and $v_2(K)$.

The distribution function $f_K(r; \lambda, N)$ of the intersegment distance r has been evaluated at the progress parameter $\lambda = 1/4$, $1/2$ and $3/4$ for random polygons under some topological constraint K [29]. However, we focus on the case of $\lambda = 1/2$. The range of intersegment distance r is divided into a number of bins of width Δr. Here we set $\Delta r = 0.25$. We enumerate the number of intersegment distances in each of the bins. The distribution function is obtained by dividing the number of each bin by the total number of intersegment distances. Similarly, we numerically evaluate the distribution $g_K(R; N)$ of gyration radius R for random polygons under some topological constraint K. Here we take $\Delta R = 0.25$.

4. Results of the simulation

4.1. Functional forms of the distributions

The asymptotic scaling form of the end-to-end distance distribution of the self-avoiding walks is derived for the region $\rho = r/N^\nu \gg 1$ [1, 30, 31]. We now apply it to the data of the distribution function for the distance between opposites nodes for random polygons under topological constraint K. We thus have the following:

$$f_K(r; \lambda, N) = A_K r^{2+\theta_K} \exp[-D_K r^{\delta_K}], \quad (8)$$

$$\theta_K = \frac{d\nu_K + 1 - \gamma_K - d/2}{1 - \nu_K}, \quad (9)$$

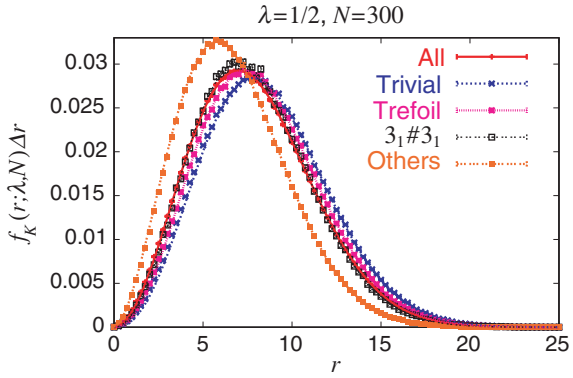

Figure 1. Distribution $f_K(r;\lambda, N)$ of intersegment distance r at $\lambda = 1/2$ for $N = 300$. Dots (·), crosses (×), asterisks (∗), open squares (□) and full squares (■) denote the plots of conditions, $all, \emptyset, 3_1, 3_1\sharp 3_1$ and others, respectively. The plots and fitting curves for $all, \emptyset, 3_1, 3_1\sharp 3_1$ and *others* are coloured with red, blue, fuchsia, black and orange, respectively.

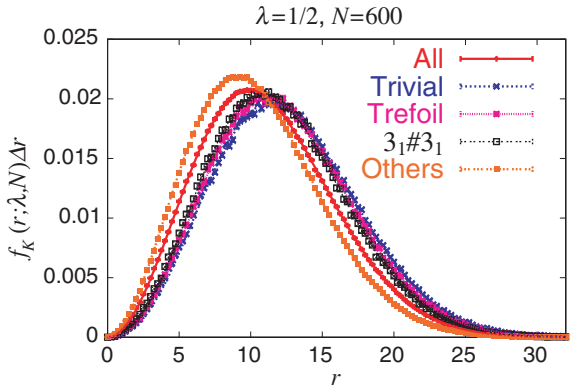

Figure 2. Distributions $f_K(r;\lambda, N)$ of intersegment distance r at $\lambda = 1/2$ for $N = 600$. Dots (·), crosses (×), asterisks (∗), open squares (□) and full squares (■) denote the plots of conditions, $all, \emptyset, 3_1, 3_1\sharp 3_1$ and *others*, respectively. The plots and fitting curves are coloured with red, blue, fuchsia, black and orange, respectively.

$$\delta_K = \frac{1}{1-\nu_K}. \tag{10}$$

Hereafter we set $d = 3$.

For the distribution $g_K(R; N)$ of gyration radius R, we introduce the following formula:

$$g_K(R; N) = A_{g,K}|R - c_K|^{\theta_{g,K}} \exp[-D_{g,K}|R - c_K|^{\delta_{g,K}}]. \tag{11}$$

For the Gaussian random walk there are some approximate expressions for the distribution of the gyration radius [35, 41]. (See also section 8 of [36].) For instance, the large R case of Fixman's result [35] corresponds to a special case of formula (11), where we set $\delta_{g,K} = 2$, $c_K = 0$ and $\theta_{g,K} = 1$.

4.2. Distribution function $f_K(r;\lambda, N)$ of intersegment distance r

The intersegment distributions $f_K(r;\lambda, N)$ at $\lambda = 1/2$ for $N = 300$ and 600 are presented in figures 1 and 2, respectively. Here the topological conditions denoted by K correspond

Table 1. The fitting values of the scaling formula (8) to the data of the distribution $f_K(r;\lambda,N)$ at $\lambda = 1/2$ with χ^2 values per datum.

N	K	γ_K	ν_K	$D_K \times 10^2$	$A_K \times 10^3$	χ^2	Fitting range
300	all	1.04 ± 0.03	0.503 ± 0.005	1.9 ± 0.1	1.78 ± 0.09	1.13	5.75–20
	$\emptyset$	0.87 ± 0.13	0.509 ± 0.019	1.7 ± 0.5	0.8 ± 0.1	1.05	6.5–16
	3_1	0.93 ± 0.09	0.50 ± 0.01	1.9 ± 0.3	1.1 ± 0.1	0.90	6.25–19
	$3_1\#3_1$	1.0 ± 0.1	0.51 ± 0.02	2.0 ± 0.6	1.5 ± 0.3	0.85	5.75–17
	others	1.1 ± 0.1	0.48 ± 0.02	2.9 ± 0.6	4.0 ± 0.5	0.81	5.5–15
600	all	1.03 ± 0.02	0.501 ± 0.004	0.99 ± 0.05	0.63 ± 0.03	0.76	7.5–30
	$\emptyset$	0.8 ± 0.2	0.51 ± 0.03	0.8 ± 0.4	0.19 ± 0.07	0.78	9–23
	3_1	0.8 ± 0.2	0.51 ± 0.02	0.9 ± 0.3	0.22 ± 0.06	1.22	8.5–23.75
	$3_1\#3_1$	1.0 ± 0.1	0.52 ± 0.02	0.7 ± 0.3	0.29 ± 0.06	0.92	7.5–22
	others	1.06 ± 0.05	0.493 ± 0.008	1.2 ± 0.1	0.94 ± 0.09	0.97	8.25–28.5

to restriction of random polygons into the following sets: (i) all polygons; (ii) polygons of the trivial knot $\emptyset$; (iii) polygons of the trefoil knot 3_1; (iv) polygons of the composite knot $3_1\sharp 3_1$ and (v) polygons of any knot types other than the three knots $\emptyset$, 3_1 and $3_1\sharp 3_1$. We thus consider the five different topological conditions. We note that the case (i) corresponds to no topological constraint. We denote the distribution functions of the five cases simply as $f_{\rm all}$, $f_\emptyset$, f_{3_1}, $f_{3_1\sharp 3_1}$ and $f_{\rm others}$, respectively.

The fitting curves of figures 1 and 2 are fit well to the data points. The curves are given by the scaling form (8), and are all very close to the Gaussian distributions. Here we note that it is also the case with the data for $\lambda = 1/4$ and $3/4$. The numerical estimates for the exponents θ_K and δ_K and the constants A_K and D_K are given in table 1. The actual ranges of distance r used for the fitting curves are also shown in table 1. The fitting curves fit very well to the data points not only in the range of r larger than the peak position but almost in the entire range of r. The χ^2 values per datum are very small. Only very small deviations are seen in the small r region, although the region is out of the fitting ranges.

The best estimates of the exponents θ_K and δ_K almost agree with the Gaussian values, i.e., $\nu_K \approx 1/2$ and $\gamma_K \approx 1$, within the range of estimation errors, for all the five different topological conditions and for both $N = 300$ and 600. The constant D_K depends on the polygonal length N. However, it does not change very much for the different knot types with respect to the estimation errors. The constant A_K depends on the knot type K for $N = 300$. However, the difference among A_Ks becomes smaller for $N = 600$ than for $N = 300$. It is thus suggested that they should become the same value when N is very large.

Let us denote by r_K^* the peak position of the distribution $f_K(r)$. Assuming the scaling form (8), the peak position r_K^* is given by

$$r_K^* = \left(\frac{2+\theta_K}{D_K\delta_K}\right)^{1-\nu_K}. \tag{12}$$

The peak position r_K^* may characterize the knot dependence of the distribution function $f_K(r)$. When $\nu_K = 0.5$ and $\gamma_K = 1.0$, the form of $f_K(r)$ is determined by the parameter D_K.

In figure 1, the peak position $r_\emptyset^*$ of the distribution $f_\emptyset(r)$ is larger than $r_{\rm all}^*$ of $f_{\rm all}$. For $f_{\rm others}$, $r_{\rm others}^*$ is smaller than $r_{\rm all}^*$. In figure 2, the peak positions of $f_\emptyset$, f_{3_1} and $f_{3_1\sharp 3_1}$ are all larger than that of $f_{\rm all}$ for $N = 600$. Their values of $N = 600$ are much closer to each other than in the case of $N = 300$. Here the peak position $r_{\rm others}^*$ of $f_{\rm others}$ is smaller than that of $f_{\rm all}$ also in the case of $N = 600$. It is thus suggested that when N is very large, the peak positions

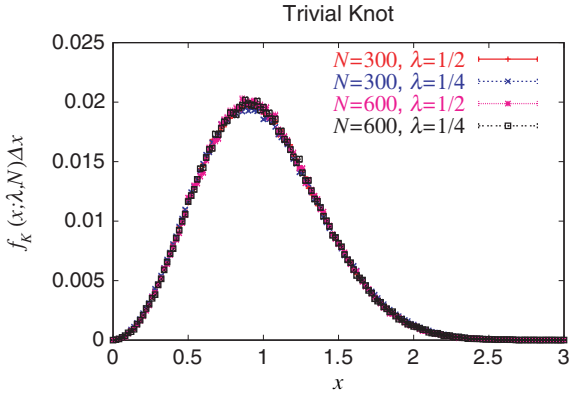

Figure 3. Distributions $\tilde{f}_{\emptyset}(x;\lambda,N)$ of normalized intersegment distance $x = r/r_K$ at $\lambda = 1/2, 1/4$ and for $N = 300, 600$. Dots $(\cdot)$, crosses $(\times)$, asterisks $(*)$ and open squares $(\square)$ denote the plots with $(\lambda, N) = (1/2, 300), (1/4, 300), (1/2, 600)$ and $(1/4, 600)$, respectively. They are displayed with red, blue, fuchsia and black, respectively. Here Δr of equation (4) is given by $\Delta x = 0.02$.

of $f_K(r)$ of simple knots should be given by the same value and the distributions $f_K(r)$ should approach a universal form.

The observations in figures 1 and 2 suggest that fixing a knot type of a random polygon leads to effective repulsion or attraction among internal segments of the polygon depending on the complexity of the knot type. When the length N becomes very large, polygons of very complex knots can appear. They should have smaller conformations than other polygons of simpler knots. As we see in figure 1 for $N = 300$, random polygons with the trivial knot have larger conformations on average than those of no topological constraints, while random polygons of more complex knots have smaller conformations. This should be consistent with the effective swelling observed in the studies on the average sizes of random polygons with some fixed knots [20, 22–24].

Let us discuss the λ and N dependence of the distribution function $f_K(r, \lambda, N)$ for a knot K. We denote by $r_K(\lambda, N)$ the average of the intersegment distance r at the parameter λ for random polygons of N nodes with the knot K. We shall suggest that for a given knot K, the distribution function $f_K(r, \lambda, N)$ should depend on N and λ only through the value $r_K(\lambda, N)$.

We introduce the distribution $\tilde{f}_K$ of normalized intersegment distance $x = r/r_K$. Here we note $\tilde{f}_K(x, \lambda, N)\,\mathrm{d}x = f_K(r, \lambda, N)\,\mathrm{d}r$. The data for the three knots show that the function $\tilde{f}_K$ does not depend on either λ or N. In figure 3, the data points of the distribution function $\tilde{f}_{\emptyset}(x; \lambda, N)$ of the normalized intersegment distance $x = r/r_{\emptyset}$ are shown for the four cases: $\lambda = 1/2$ or $1/4$ and $N = 300$ or 600. It is clear that the data points for all the four cases are located on the same curve. The best estimates of the fitting parameters to the data of $\tilde{f}_K$ are given in tables 2 and 3 for $\lambda = 1/2$ and $1/4$, respectively. As far as the five topological conditions are concerned, each of the fitting parameters of a condition K has almost the same value for $N = 300$ or 600 and for $\lambda = 1/2$ or $1/4$. Thus, we suggest that for a given knot K the distribution of the normalized intersegment distance, $\tilde{f}_K(x, \lambda, N)$, should be given by the same Gaussian form for any N and λ.

We now show that the λ and N dependence of the average distance $r_K(\lambda, N)$ is given by the Gaussian one in the cases of $\lambda = 1/4$, $1/2$ and $3/4$ for the three knots. Let us denote by $P(\mathbf{r}; N)$ the end-to-end distance distribution of the Gaussian random walk of N steps. For random polygons consisting of two Gaussian chains of λN steps and $(1 - \lambda)N$ steps, the

Table 2. The fitting values of the scaling formula (8) to the data of the re-scaled distribution $\tilde{f}_K(x; \lambda, N)$ at $\lambda = 1/2$ with χ^2 values per datum.

N	K	γ_K	ν_K	D_K	$A_K \times 10^2$	χ^2	Fitting range
300	all	1.04 ± 0.04	0.504 ± 0.006	1.25 ± 0.04	6.3 ± 0.2	0.80	0.70–2.00
	$\emptyset$	0.89 ± 0.08	0.51 ± 0.01	1.39 ± 0.08	7.7 ± 0.6	1.20	0.70–2.00
	3_1	0.99 ± 0.08	0.52 ± 0.01	1.30 ± 0.08	6.9 ± 0.5	0.89	0.70–2.00
	$3_1\#3_1$	1.1 ± 0.1	0.52 ± 0.02	1.2 ± 0.1	6.4 ± 0.8	0.90	0.70–2.00
	others	1.04 ± 0.07	0.49 ± 0.01	1.26 ± 0.07	6.2 ± 0.4	0.91	0.70–2.00
600	all	1.03 ± 0.04	0.502 ± 0.006	1.26 ± 0.04	6.4 ± 0.2	0.75	0.70–2.00
	$\emptyset$	1.0 ± 0.1	0.53 ± 0.02	1.3 ± 0.1	7.2 ± 0.8	0.81	0.70–2.00
	3_1	0.9 ± 0.1	0.51 ± 0.02	1.4 ± 0.1	7.8 ± 1.0	1.26	0.70–2.00
	$3_1\#3_1$	1.0 ± 0.1	0.52 ± 0.02	1.3 ± 0.1	7.2 ± 1.0	1.05	0.70–2.00
	others	1.06 ± 0.05	0.499 ± 0.008	1.24 ± 0.05	6.2 ± 0.3	1.00	0.70–2.00

Table 3. The fitting values of the scaling formula (8) to the data of the re-scaled distribution $\tilde{f}_K(x; \lambda, N)$ at $\lambda = 1/4$ with χ^2 values per datum.

N	K	γ_K	ν_K	D_K	$A_K \times 10^2$	χ^2	Fitting range
300	all	1.10 ± 0.04	0.514 ± 0.006	1.19 ± 0.04	6.0 ± 0.2	0.88	0.70–2.00
	$\emptyset$	1.01 ± 0.09	0.52 ± 0.01	1.28 ± 0.08	6.8 ± 0.6	1.54	0.70–2.00
	3_1	1.15 ± 0.07	0.54 ± 0.01	1.14 ± 0.07	5.9 ± 0.4	0.94	0.70–2.00
	$3_1\#3_1$	1.0 ± 0.2	0.51 ± 0.02	1.3 ± 0.2	6.8 ± 1.0	1.06	0.70–2.00
	others	1.11 ± 0.07	0.50 ± 0.01	1.20 ± 0.07	5.8 ± 0.4	1.03	0.70–2.00
600	all	1.05 ± 0.05	0.507 ± 0.007	1.24 ± 0.05	6.2 ± 0.3	1.28	0.70–2.00
	$\emptyset$	1.0 ± 0.1	0.53 ± 0.02	1.3 ± 0.1	7.0 ± 0.7	0.78	0.70–2.00
	3_1	0.8 ± 0.1	0.50 ± 0.02	1.4 ± 0.1	8.1 ± 1.1	1.24	0.70–2.00
	$3_1\#3_1$	0.9 ± 0.2	0.51 ± 0.02	1.4 ± 0.1	7.5 ± 1.1	1.18	0.70–2.00
	others	1.13 ± 0.05	0.511 ± 0.008	1.17 ± 0.05	5.8 ± 0.3	1.07	0.70–2.00

probability distribution of the vector $\mathbf{r}$ connecting the two end-points should be proportional to the product $P(\mathbf{r}; \lambda N)P(\mathbf{r}; (1-\lambda)N)$. Here we note that the intersegment vector $\mathbf{r}$ for the parameter λ connects the common end-points of the two random walks of length λN and $(1-\lambda)N$. For the case of no topological constraint, therefore, the constant $D_{\rm all}$ is given by

$$D_{\rm all} = \frac{3}{2\lambda(1-\lambda)Na^2}. \tag{13}$$

Here a denotes the bond length, and $a = 1$ in this paper. We thus have

$$r_{\rm all}(\lambda, N) = \sqrt{\frac{8}{3\pi}}\sqrt{\lambda(1-\lambda)N}a. \tag{14}$$

The ratio $r_K(\lambda, N)/r_{\rm all}(\lambda, N)$ is plotted in figure 4 for $N = 300$ and 600 with respect to the topological conditions, $\emptyset$, 3_1, $3_1\sharp 3_1$ and others. In each case of the four topological conditions, the ratio takes almost the same value for $\lambda = 1/2$, $1/4$ and $3/4$. Furthermore, we find that the ratio should also coincide with the ratio of the gyration radii, $R_K/R_{\rm all}$. Thus, we have the conjecture: $r_K(\lambda, N) = r_{\rm all}(\lambda, N)R_K/R_{\rm all}$. If the conjecture is true, then the λ dependence of the distribution $f_K(r, \lambda, N)$ is completely given by the Gaussian one, and the N dependence is given by the Gaussian with the re-scaling factor $R_K/R_{\rm all}$. Here we remark that the ratio $R_K/R_{\rm all}$ may depend on the number of nodes N, since random polygons under a topological

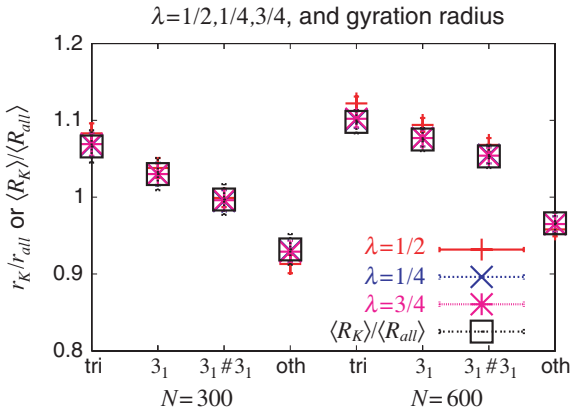

Figure 4. The ratio of the average distances $r_K/r_{\rm all}$ and that of the gyration radii $\langle R_K\rangle/\langle R_{\rm all}\rangle$ for a given topological condition K. The ratios $r_K(\lambda, N)/r_{\rm all}(\lambda, N)$ for $\lambda = 1/2$, $1/4$ and $3/4$ are denoted by dots $(\cdot)$, crosses $(\times)$ and asterisks $(*)$, respectively. Here K is given by $\emptyset$, 3_1, $3_1\sharp 3_1$ and *others* (oth). The ratio $\langle R_K\rangle/\langle R_{\rm all}\rangle$ is denoted by open squares $(\square)$ for the four cases of K. Here we consider $N = 300$ and 600. Dots, crosses, asterisks and squares are coloured with red, blue, fuchsia and black, respectively.

constraint can be larger or smaller than that of no topological constraint due to entropic repulsion induced by the topological constraint.

We explain some details about the average size of random polygons. We first recall that the symbol R_K denotes the square root of the mean square radius of gyration for random polygons of a topological constraint K. We denote by $\langle R_K\rangle$ the mean gyration radius of a polygon averaged over an ensemble of random polygons of a topological constraint K. In figure 4, the ratio $\langle R_K\rangle/\langle R_{\rm all}\rangle$ is plotted for the four topological conditions. However, the difference between the two ratios, $R_K/R_{\rm all}$ and $\langle R_K\rangle/\langle R_{\rm all}\rangle$, should be smaller than the error bars.

Let us discuss the knot dependence of the distribution f_K. We show that the distribution $\tilde{f}_K$ of the normalized distance x for a knot K should be almost independent of the knot type. In figure 5, the re-scaled distribution $\tilde{f}_K$ for the five topological conditions are plotted against the normalized intersegment distance $x = r/r_K$ for the case of $N = 300$ and $\lambda = 1/2$. We see in figure 5 that the distributions $\tilde{f}_K$ should almost the same for the three knots. It is consistent with the observation that the estimates of the parameters are of similar values for the five topological conditions, as shown in tables 2 and 3. Thus, the knot dependence of the distribution f_K should be renormalized into the value $r_K(\lambda, N)$.

4.3. Distribution $g_K(R; N)$ of gyration radius R

The distribution functions $g_K(R; N)$ of gyration radius R are shown in figures 6 and 7 with respect to the five topological conditions for $N = 300$ and 600, respectively. Here the five cases are the same as in section 4.2. We denote the distributions g_K for the five cases briefly as $g_{\rm all}$, $g_\emptyset$, g_{3_1}, $g_{3_1\sharp 3_1}$ and $g_{\rm others}$, respectively. The fitting curves in figures 6 and 7 fit well to the data points in some ranges of R. The curves are given by formula (11). Thus, formula (11) approximates the distribution $g_K(R; N)$ of gyration radius effectively. They could be useful for studying topological effects on the gyration radius.

Let us consider plotting the distribution g_K with respect to a normalized variable of the gyration radius, R/R_K. More precisely, we consider plotting g_K in terms of the variable

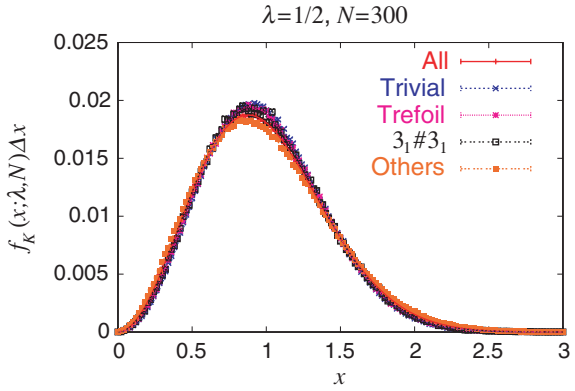

Figure 5. Distribution $\tilde{f}_K(x;\lambda,N)$ of normalized intersegment distance $x = r/r_K$ for $\lambda = 1/2$ and $N = 300$. The distributions $\tilde{f}_K(x;\lambda,N)$ for *all*, $\emptyset$, 3_1, $3_1\sharp 3_1$ and *others* are denoted by dots ($\cdot$), crosses ($\times$), asterisks ($*$), open squares ($\square$) and full squares ($\blacksquare$), respectively. The plots and fitting curves are coloured with red, blue, fuchsia, black and orange, respectively. Here Δr of equation (4) is given by $\Delta x = 0.02$.

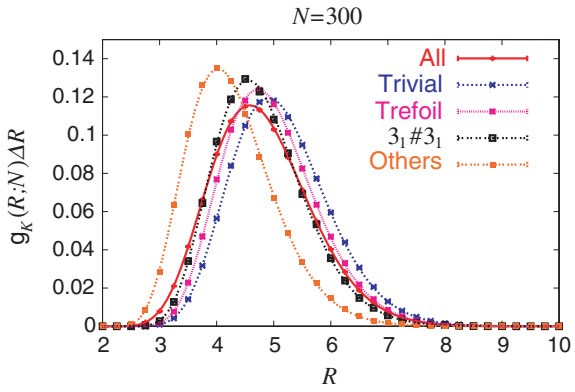

Figure 6. Distribution $g_K(R;N)$ of gyration radius R for $N = 300$. Dots ($\cdot$), crosses ($\times$), asterisks ($*$), open squares ($\square$) and full squares ($\blacksquare$) denote the distribution $g_K(R;N)$ for *all*, $\emptyset$, 3_1, $3_1\sharp 3_1$ and *others*, respectively. The plots and fitting curves are coloured with red, blue, fuchsia, black and orange, respectively.

$R/\langle R_K\rangle$. Here we recall that $\langle R_K\rangle$ denotes the average of the gyration radius of a polygon averaged over an ensemble of random polygons with a given knot K. We introduce distribution $\tilde{g}_K(y;N)$ of the variable $y = R/\langle R_K\rangle$ by the relation: $\tilde{g}_K(y;N)\,\mathrm{d}y = g_K(R;N)\,\mathrm{d}R$. Hereafter, however, we denote $\langle R_K\rangle$ simply by R_K, except for figure captions.

We now present the re-scaled distribution $\tilde{g}_K$ in figures 8 and 9 for $N = 300$ and $N = 600$, respectively. We find that for a given knot K the distribution $\tilde{g}_K$ of normalized gyration radius $y = R/R_K$ should be independent of the knot type almost completely. In figures 8 and 9, the data points and their fitting curves of $\tilde{g}_K$ overlap each other for the cases of the three knots, $\emptyset$, 3_1 and $3_1\sharp 3_1$. We also find that the fitting curves fit well to the data points both in figures 8 and 9. They are drawn by a fitting formula corresponding to (11)

$$\tilde{g}_K(y;N) = \tilde{A}_{g,K}|y-\tilde{c}_K|^{\theta_{g,K}}\exp[-\tilde{D}_{g,K}|y-\tilde{c}_K|^{\delta_{g,K}}]. \tag{15}$$

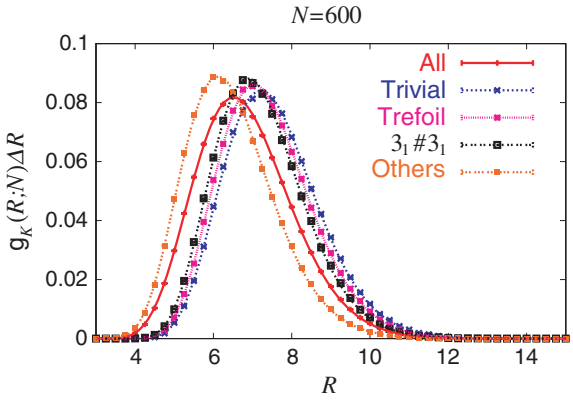

Figure 7. Distribution $g_K(R; N)$ of gyration radius R for $N = 600$. Dots (·), crosses (×), asterisks (∗), open squares (□) and full squares (■) denote the distribution $g_K(R; N)$ for *all*, $\emptyset$, 3_1, $3_1\sharp 3_1$ and *others*, respectively. The plots and fitting curves are coloured with red, blue, fuchsia, black and orange, respectively.

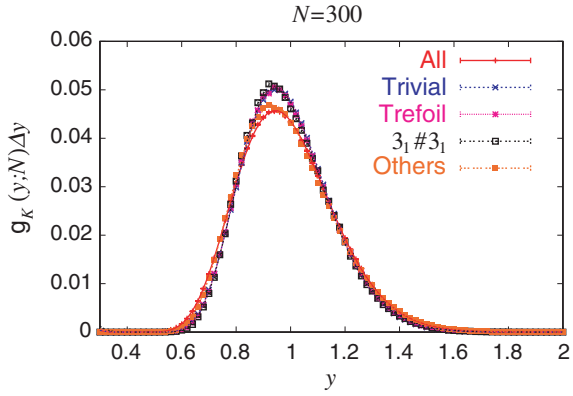

Figure 8. Distribution $\tilde{g}_K(y; N)$ of the normalized gyration radius $y = R/\langle R_K \rangle$ for $N = 300$. Dots (·), crosses (×), asterisks (∗), open squares (□) and full squares (■) denote the distribution $\tilde{g}_K(y; N)$ for the conditions, *all*, $\emptyset$, 3_1, $3_1\sharp 3_1$ and *others*, respectively. The plots and fitting curves are coloured with red, blue, fuchsia, black and orange, respectively. Here ΔR of equation (7) is given by $\Delta y = 0.02$.

The fitting parameters $\tilde{A}_{g,K}$, $\tilde{D}_{g,K}$ and $\tilde{c}_K$ correspond to $A_{g,K}$, $D_{g,K}$ and c_K of formula (11) as

$$A_{g,K} = \tilde{A}_{g,K} \big/ R_K^{1+\theta_{g,K}}, \qquad D_{g,K} = \tilde{D}_{g,K} \big/ R_K^{\delta_{g,K}}, \qquad c_K = \tilde{c}_K R_K. \tag{16}$$

The best estimates of the fitting parameters are listed in table 4. The χ^2 values are good, in particular, for the cases of the three knots, $\tilde{g}_\emptyset$, $\tilde{g}_{3_1}$ and $\tilde{g}_{3_1\sharp 3_1}$. Here the fitting range of $y = R/R_K$ is given by 0.4–2.0 for all the fitting parameters given in table 4.

The knot dependence and the N dependence of distribution g_K should be renormalized into the mean square radius of gyration, $R_K^2(N)$. The re-scaled distributions $\tilde{g}_K$ for the three knots do not depend on the polygonal length, N. The fitting curves of $\tilde{g}_K$ for the three knots are almost the same for $N = 300$ and $N = 600$. We can confirm the observation in figures 8 and 9 by comparing the estimates shown in table 4. The fitting parameters $\theta_{g,K}$, $\delta_{g,K}$, $\tilde{A}_{g,K}$ and $\tilde{c}_K$ depend on neither the knot type K nor the polygonal length N with respect to their

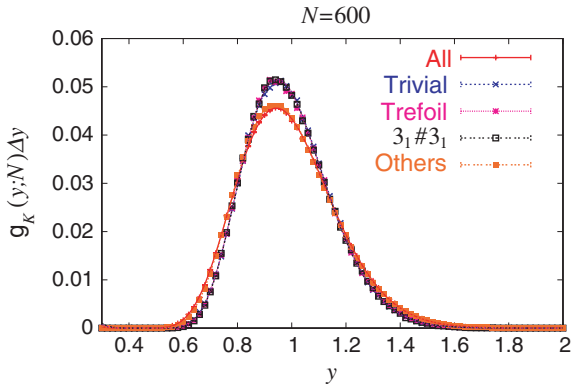

Figure 9. Distribution $\tilde{g}_K(y; N)$ of the normalized gyration radius $y = R/R_K$ for $N = 600$. Dots (·), crosses (×), asterisks (∗), open squares (□) and full squares (■) denote the distribution $\tilde{g}_K(y; N)$ for the conditions, *all*, ∅, 3_1, $3_1\sharp 3_1$ and *others*, respectively. The plots and fitting curves are coloured with red, blue, fuchsia, black and orange, respectively. Here ΔR of equation (7) is given by $\Delta y = 0.02$.

Table 4. The fitting values of formula (15) to the data of the re-scaled distribution $\tilde{g}_K(y; N)$ of the normalized gyration radius $y = R/\langle R_K \rangle$ for N-noded random polygons of topological condition K with χ^2 values per datum. The fitting range of y is from 0.4 to 2.0.

N	K	$\theta_{g,K}$	$\delta_{g,K}$	$\tilde{D}_{g,K}$	$\tilde{A}_{g,K} \times 10^{-4}$	$\tilde{c}_K$	χ^2
300	all	6.2 ± 0.3	1.44 ± 0.03	11.0 ± 0.4	0.019 ± 0.009	0.423 ± 0.007	3.63
	∅	7.9 ± 0.4	1.31 ± 0.03	14.6 ± 0.6	0.4 ± 0.3	0.441 ± 0.006	1.61
	3_1	8.3 ± 0.3	1.21 ± 0.03	16.1 ± 0.6	1.7 ± 1.1	0.450 ± 0.004	3.33
	$3_1\#3_1$	8.7 ± 0.5	1.13 ± 0.03	17.3 ± 0.8	6 ± 5	0.457 ± 0.005	1.16
	others	7.7 ± 0.3	1.12 ± 0.03	15.1 ± 0.6	1.1 ± 0.6	0.441 ± 0.004	3.97
600	all	6.2 ± 0.3	1.42 ± 0.02	11.0 ± 0.3	0.020 ± 0.007	0.424 ± 0.006	5.91
	∅	7.7 ± 0.3	1.30 ± 0.03	14.9 ± 0.4	0.46 ± 0.23	0.457 ± 0.005	1.86
	3_1	8.3 ± 0.3	1.21 ± 0.03	16.3 ± 0.5	1.9 ± 1.1	0.458 ± 0.004	2.39
	$3_1\#3_1$	8.1 ± 0.3	1.22 ± 0.03	16.0 ± 0.5	1.3 ± 0.6	0.463 ± 0.003	2.38
	others	7.0 ± 0.3	1.25 ± 0.03	13.1 ± 0.5	0.14 ± 0.08	0.434 ± 0.006	6.90

errors. The normalization of gyration radius, R/R_K, should be thus essential when analysing the distribution function g_K.

Random polygons of relatively simple knots should be larger in size than the average one, while those of more complex knots should be smaller. It depends on the polygonal length N whether the size of random polygons of a given knot should be larger or smaller than the average. In figure 6, the peak position of the distribution $g_\emptyset$ is larger than those of the other distributions $g_{\rm all}$, g_{3_1}, $g_{3_1\sharp 3_1}$ and $g_{\rm others}$. In figure 7, the peaks of $g_\emptyset$, g_{3_1}, $g_{3_1\sharp 3_1}$ are clearly located on the right-hand side of the peak of $g_{\rm all}$, while the peak of $g_{\rm others}$ is located on the left-hand side. The equilibrium length of a random knot can be a criterion whether it is larger or smaller than the average [42]. We also note that the peak positions of distributions g_K shown in figures 6 and 7 are roughly consistent with the average values of R_K [20, 22–24].

5. Discussion

We have found that the distribution f_K of intersegment distance for random polygons under topological constraint K is almost given by the Gaussian distribution. Furthermore, re-scaling

the distance by the average distance r_K, we have shown that the λ and N dependence of f_K is renormalized into the average distance $r_K(\lambda, N)$. We have proposed the conjecture: $r_K = r_{\rm all} R_K / R_{\rm all}$, for any λ, N and K. Here we have assumed that N is large enough. If it is true, then topological constraints do not have any effect on the distribution of intersegment distance, f_K, except for scaling the distance by the factor $R_K / R_{\rm all}$.

The effect of the 'topological excluded volume' should be rather different from the standard excluded volume effect of self-avoiding walks. It does not correspond to a real excluded volume, although the ratio $R_K / R_{\rm all}$ of a knot K can become larger than 1 in the case of large N. When N increases, random polygons with more complex knots can appear, which should be smaller than those of a simple knot. If we consider only such random polygons that have a fixed simple knot, then the size can be larger than the average one when N is very large. Topological constraints thus may induce effective swelling of random polygons. However, they do not change the functional form of the distribution of the distance between two segments.

Let us discuss the difference in terms of critical exponents. We denote by ν'_K the scaling exponent defined for the asymptotic behaviour of the average size of SAW such as given in (1). For SAW, the exponent ν'_K corresponds to the exponent ν_K determined by formula (8) [1]. If des Cloizeaux's relations (9) and (10) could be valid for random polygons under topological constraints, we should have $\nu'_K \simeq 0.50$ from the best estimates for the distribution $f_K(r; \lambda, N)$ as shown in table 1.

Within the scope of this research, however, it is not clear whether two exponents ν_K and ν'_K should be equal or not. Moreover, it is not clear whether relations (9) and (10) should be valid for random polygons under topological constraints. It seems that the form of the distribution $f_K(r; \lambda, N)$ remains Gaussian with the exponent $\nu_K \simeq 0.50$ in the limit $N \to \infty$. However, the average size $R_K^2(N)$ might follow the scaling form with a different exponent, $\nu'_K > 0.5$.

Acknowledgments

The authors are grateful to M K Shimamura for helpful discussions. AY was supported in part by the Chuo University.

References

[1] des Cloizeaux J 1974 *Phys. Rev.* A **10** 1665–9
[2] Shaw S Y and Wang J C 1993 *Science* **260** 533
[3] Rybenkov V V, Cozzarelli N R and Vologodskii A V 1993 *Proc. Natl. Acad. Sci. USA* **90** 5307
[4] Delbrück M 1962 *Proc. Symp. Appl. Math.* **4** 55–63
[5] Frisch H L and Wasserman E 1961 *J. Am. Chem. Soc.* **83** 3789
[6] Vologodskii A V, Lukashin A V, Frank-Kamenetskii M D and Anshelevich V V 1974 *Sov. Phys. JETP* **39** 1059–63
[7] Michels J P J and Wiegel F W 1982 *Phys. Lett.* A **90** 381–4
[8] des Cloizeaux J and Metha M L 1979 *J. Phys.* **40** 665–70
[9] Sumners D W and Whittington S G 1988 *J. Phys. A: Math. Gen.* **21** 1689–94
[10] Pippenger N 1989 *Disc. Appl. Math.* **25** 273–8
[11] Koniaris K and Muthukumar M 1991 *Phys. Rev. Lett.* **66** 2211–4
[12] Deguchi T and Tsurusaki K 1994 *J. Knot Theory Ramifications* **3** 321–53
[13] Deguchi T and Tsurusaki K 1997 Random knots and links and applications to polymer physics *Lectures at Knots'96* ed S Suzuki (Singapore: World Scientific) 95–122
[14] Shimamura M K and Deguchi T 2001 *J. Phys. Soc. Japan* **70** 1523–36
[15] Dobay A, Sottas P-E, Dubochet J and Stasiak A 2001 *Lett. Math. Phys.* **55** 239

[16] Orlandini E, Tesi M, Janse van Rensburg E J and Whittington S G 1998 *J. Phys. A: Math. Gen.* **31** 5953–67
[17] Shimamura M K and Deguchi T 2002 *Phys. Rev.* E **65** 051802
[18] Shimamura M K and Deguchi T 2003 *Phys. Rev.* E **68** 061108
[19] des Cloizeaux J 1981 *J. Phys. Lett. (France)* **42** L433–L436
[20] Deutsch J M 1999 *Phys. Rev.* E **59** R2539–41
[21] Grosberg A Yu 2000 *Phys. Rev. Lett.* **85** 3858
[22] Shimamura M K and Deguchi T 2002 *J. Phys. A: Math. Gen.* **35** L241–L246
[23] Matsuda H, Yao A, Hiroshi T, Deguchi T, Furuta K and Inami T 2003 *Phys. Rev.* E **68** 011102
[24] Dobay A, Dubochet J, Millet K, Sottas P E and Stasiak A 2003 *Proc. Natl. Acad. Sci. USA* **100** 5611–5
[25] Grosberg A Yu 2003 *Les Diablerets (Switzerland, 14–17 July)*
[26] de Gennes P G 1979 *Scaling Concepts in Polymer Physics* (New York: Cornell University Press)
[27] Bishop M and Clarke J H R 1991 *J. Chem. Phys.* **94** 3936–42
[28] Bishop M and Clarke J H R 1991 *J. Chem. Phys.* **95** 4589–92
[29] Yao A 2004 Topological effects on statistical mechanical properties of ring polymers (in Japanese) *PhD Thesis* Chuo University
[30] Fisher M E 1966 *J. Chem. Phys.* **44** 616–22
[31] McKenzie D S and Moore M A 1971 *J. Phys. A: Gen. Phys.* **4** L82–6
[32] Lipkin M, Oono Y and Freed K F 1981 *Macromolecules* **14** 1270–7
[33] Caracciolo S, Causo M S and Plissetto A 2000 *J. Chem. Phys.* **112** 7693–710
[34] Lue L and Kiselev S B 1999 *J. Chem. Phys.* **110** 2684–91
[35] Fixman M 1962 *J. Chem. Phys.* **36** 306–10
[36] Yamakawa H 1971 *Modern Theory of Polymer Solutions* (New York: Harper and Row)
[37] Freire J J and Horta A 1976 *J. Chem. Phys.* **65** 4049–54
[38] Yao A, Matsuda H, Tsukahara H, Shimamura M K and Deguchi T 2001 *J. Phys. A: Math. Gen.* **34** 7563–77
[39] Deguchi T and Tsurusaki K 1993 *Phys. Lett.* A **174** 29–37
[40] Polyak M and Viro O 1994 *Int. Math. Res. Not.* **11** 445–53
[41] Flory F J and Fisk S 1966 *J. Chem. Phys.* **44** 2243–8
[42] Diao Y, Dobay A, Kusner R B, Millett K and Stasiak A 2003 *J. Phys. A: Math. Gen.* **36** 11561–74